Cell Reports, Volume *14*

Supplemental Information

The Microcephaly-Associated Protein Wdr62/CG7337 Is Required to Maintain Centrosome Asymmetry in *Drosophila* Neuroblasts

Anjana Ramdas Nair, Priyanka Singh, David Salvador Garcia, David Rodriguez-Crespo, Boris Egger, and Clemens Cabernard

Supplemental Information

Supplemental Data

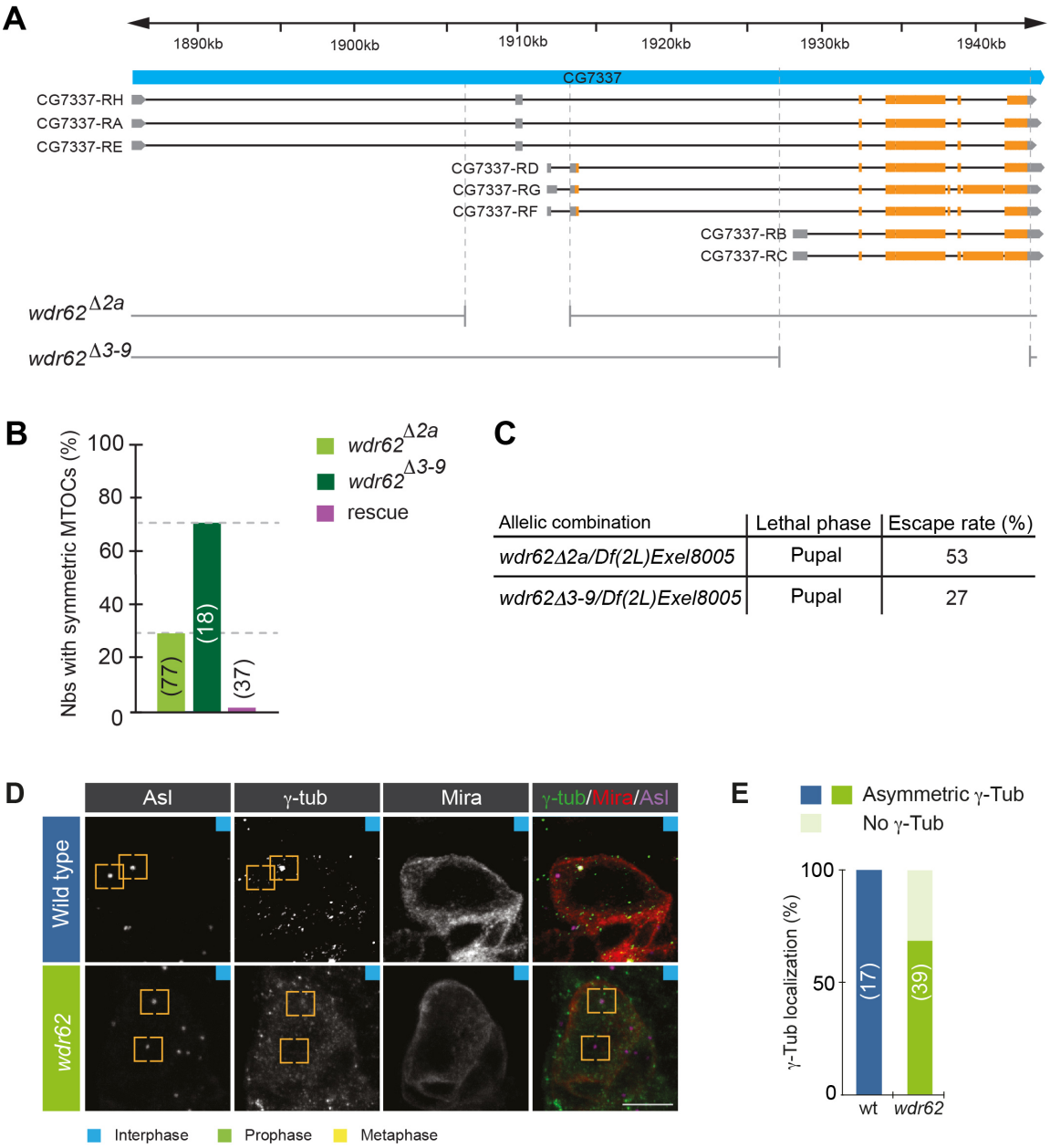

Figure S1: *wdr62* locus and alleles, related to Figure 1

(A) Locus map of *CG7337/wdr62*. Orange bars represent the predicted coding region. *wdr62* alleles are indicated below; molecularly defined breakpoints are highlighted with vertical dashed lines. **(B)** Phenotypic penetrance of the generated *wdr62* alleles. The centrosome asymmetry phenotype of *wdr62*$^{\Delta 2a}$ was fully rescued by expressing *UAS-CG7337::mDendra2*. **(C)** Table indicating lethal phase and number of escapers for *wdr62*$^{\Delta 2a}$ and *wdr62*$^{\Delta 3-9}$ crossed over the deficiency *Df(2L)Exel8005*. This deficiency removes the entire CG7337 locus plus adjacent genes (not shown in (a)). **(D)** Representing confocal images of wild type and *wdr62* mutant (*wdr62*$^{\Delta 2a}$ */Df(2L)Exel8005*) neuroblasts stained for the centriolar marker Asterless (Asl; magenta in overlay), γ-tubulin (γ-tub; green in overlay) and the neuroblast marker Miranda (Mira; red in overlay). Yellow brackets highlight neuroblast centrosomes. **(E)** Quantification of the centrosome asymmetry phenotype in the immunohistochemistry experiment. Number of scored neuroblasts (n's) is indicated on the bar graphs. Colored boxes refer to the corresponding cell cycle stage. Scale bar is 5 μm.

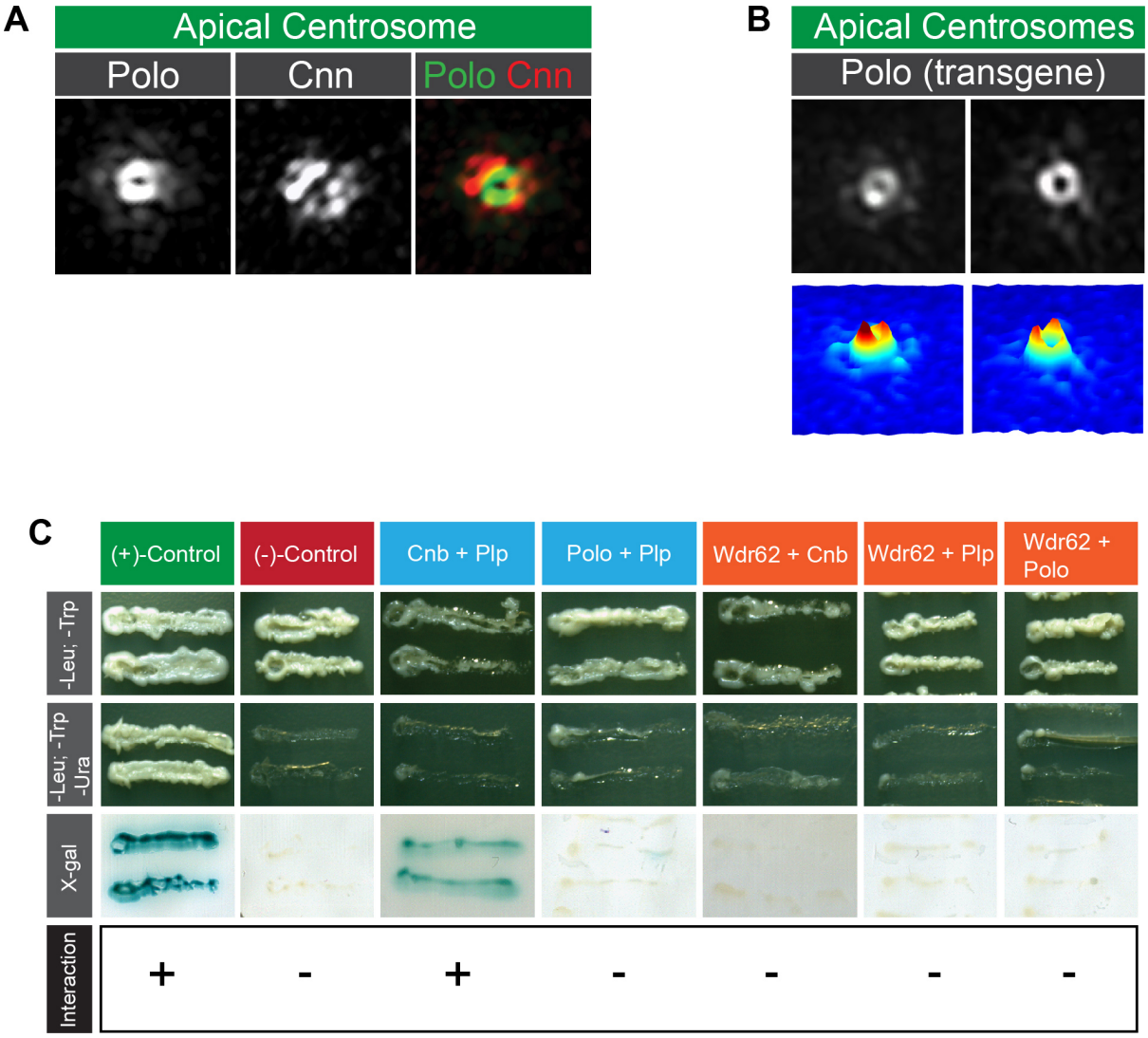

Figure S2: Wdr62 is required for Polo's association with the PCM, related to Figure 2&3
(A) Representative image of an apical wild type interphase centrosome expressing Polo fused to GFP. In this line, the GFP cassette is inserted into Polo's coding region, resulting in an in-frame fusion between Polo's exons and GFP (Protein trap line). The neuroblast was stained for Cnn (white in single channel and red in overlay). **(B)** Representative image of an apical wild type centrosome expressing Polo::GFP, encoded by a transgene. In this line, Polo's cDNA has been fused to GFP and combined with its own regulatory elements. Note that both Polo::GFP lines (protein trap in (a) and transgenic line in (b)) show the pool of Polo associated with the PCM. **(C)** Yeast-two Hybrid experiments, testing for direct molecular interactions between Cnb, Polo and Wdr62. Positive and negative controls are on the left. Positive interactions are denoted with a (+), negative interactions with a (-). See Experimental procedures for details.

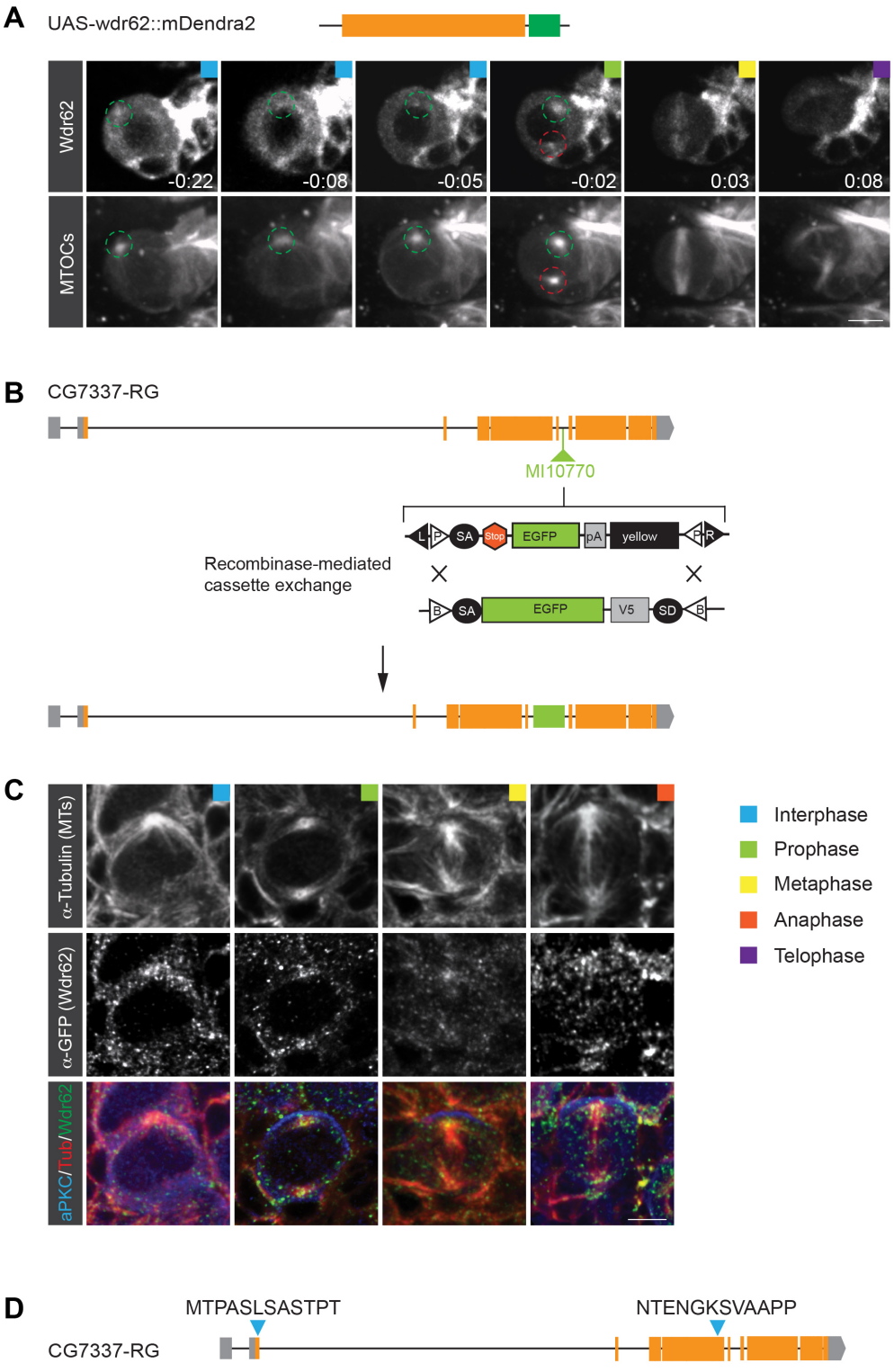

Figure S3: Wdr62 is a MT-associated protein, related to Figure 4
(A) Image sequence of a wild type neuroblast, expressing *UAS-CG7337::mDendra2*, driven by the neuroblast specific *worGal4* driver line. **(B)** The coding region of the longest *CG7337/wdr62* isoform, highlighting the location of the MiMIC cassette (green triangle), amenable for recombination mediated cassette exchange (RMCE). **(C)** Representative wild type neuroblast, expressing *wdr62::EGFP* (MiMIC line; in-frame fusion of GFP inserted into intron as shown in (b)), stained for a-GFP (green in overlay), alpha-Tubulin (red in overlay) and aPKC (blue in overlay). **(D)** The coding region of the longest *CG7337/wdr62* isoform, highlighting the locations (blue triangles) and sequence of the epitopes used to generate peptide antibodies. Colored boxes refer to cell cycle stages. Time in h:min; Scale bar is 5 μm.

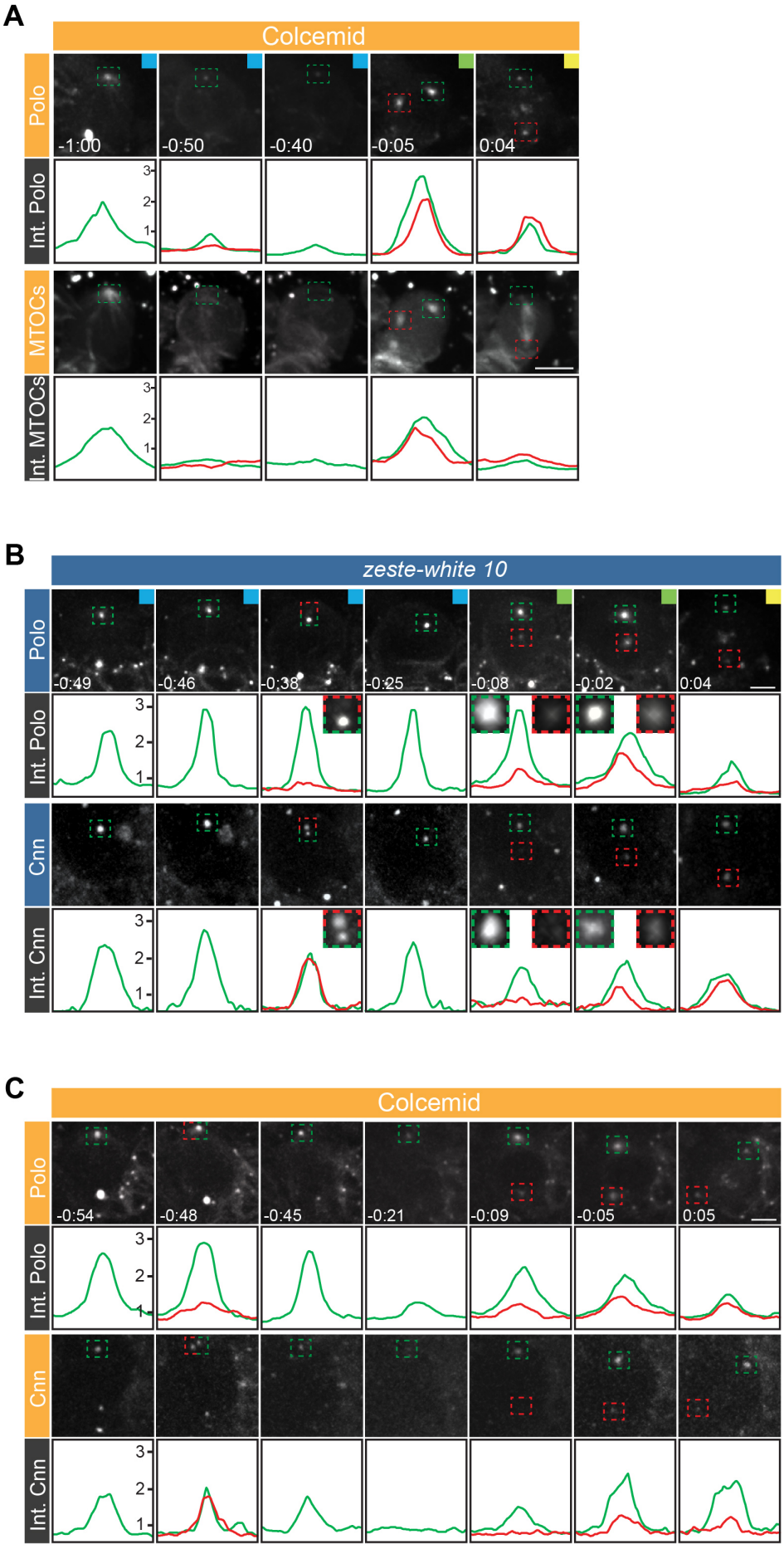
A
Colcemid
Polo
-1:00
-0:50
-0:40
-0:05
0:04
Int. Polo
MTOCs
Int. MTOCs
B
zeste-white 10
Polo
-0:49
-0:46
-0:38
-0:25
-0:08
-0:02
0:04
Int. Polo
Cnn
Int. Cnn
C
Colcemid
Polo
-0:54
-0:48
-0:45
-0:21
-0:09
-0:05
0:05
Int. Polo
Cnn
Int. Cnn

Figure S4: microtubules are required to maintain Polo and Cnn on the apical interphase centrosome, related to Figure 4

(A) Representative *zeste-white 10* mutant neuroblasts expressing Polo::GFP and the MTOC marker Jupiter::mCherry or **(C)** Cnn::mCherry exposed to low doses of colcemid. **(B)** Representative control image sequence of a *zeste-white 10* mutant neuroblast expressing Polo::GFP (top row) and the PCM marker Cnn::mCherry (bottom row). In all panels, the green and red lines below the image sequences represent Cnn, Polo or MT intensity values of the apical (green box) and basal (red box) centrosomes, respectively. Inserts show high magnification of the apical and basal centrosome for selected time points. Contrast and brightness has been adjusted for better visibility. Time in h:min; Scale bar is 5 μm.

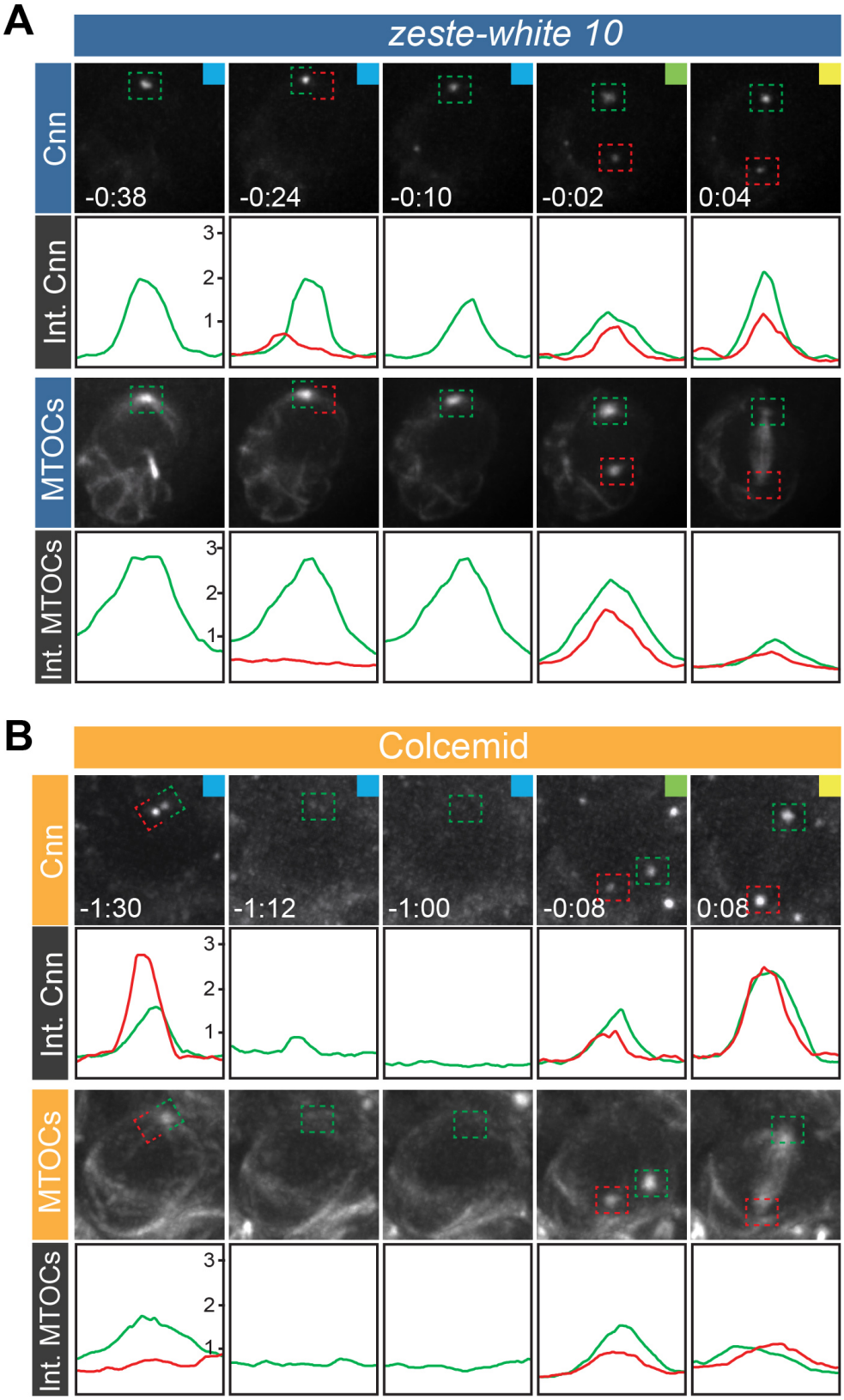

Figure S5: Loss or gain of Cnn correlates with Polo localization, related to Figure 4
(A) Representative *zeste-white 10* mutant control neuroblast expressing Polo::GFP and the MTOC marker Jupiter::mCherry. **(B)** *zeste-white 10* mutant neuroblast expressing Polo::GFP and the MTOC marker Jupiter::mCherry exposed to low doses of colcemid. The green and red lines below the image sequences represent Polo and MTOC intensity values of the apical (green box) and basal (red box) centrosomes, respectively. Time in h:min; Scale bar is 5 μm.

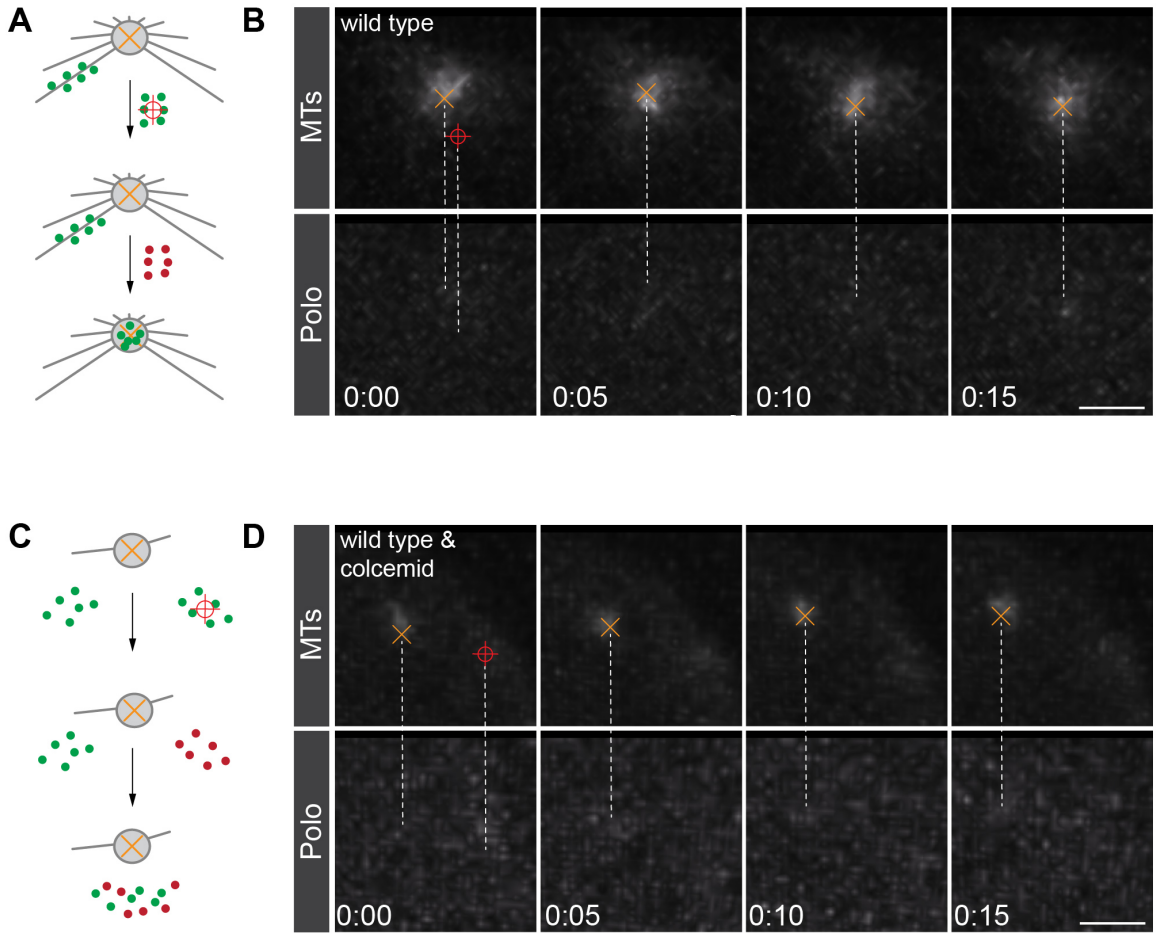

Figure S6: Polo is traveling on MTs to the centrosome center, related to Figure 5
(A) Cartoon illustrating a control photoactivation experiment in wild type neuroblasts. Green balls represent unconverted Polo::mDendra2 molecules localized to astral MTs (grey lines) or in the cytoplasm (white background). The red crosshair indicates the target area. **(B)** Representative image sequence of a wild type neuroblast expressing the microtubule marker G147 (MTs; top row; white) and Polo::mDendra2 (photoconverted in bottom row (white)). Red crosshairs represent the target area that was photoconverted. For this control experiment, the cytoplasm was targeted. Note that essentially no photoconverted Polo is detectable. **(C)** Cartoon illustrating a control photoactivation experiment in colcemid treated wild type neuroblasts. **(D)** Representative image sequence of a wild type, colcemid treated neuroblast expressing the microtubule marker G147 (MTs; top row; white) and Polo::mDendra2 (photoconverted in bottom row (white)). Note that MTs were not completely depolymerized. Yellow crosses represent the center of the centrosome. Time in h:min; Scale bar is 5 μm.

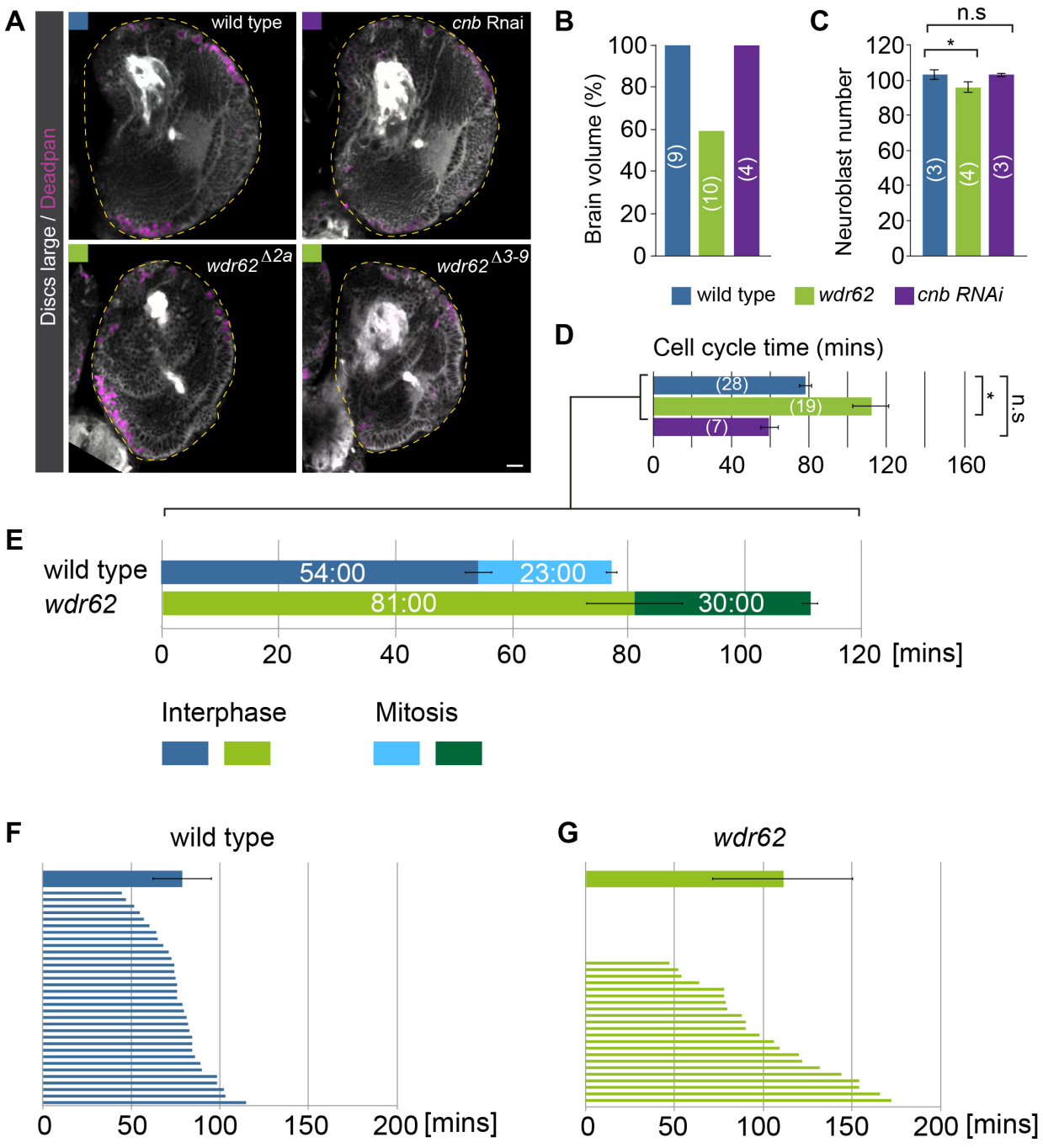

Figure S7: *wdr62* mutant brains are decreased in size due to cell cycle defects, related to Figure 7
(A) Sections of representative third instar brain lobes for the indicated genotypes and labeled with the cell membrane marker discs large (Dlg; white) and the neuroblast marker Deadpan (Dpn; magenta). **(B)** Brain volumes of wild type, *wdr62* and *cnb* RNAi are displayed as a percentage. **(C)** Neuroblast number and **(D)** cell cycle times are shown for the indicated genotypes (*wdr62*$^{\Delta 3\text{-}9}$*/Df(2L)Exel8005)*. **(E)** Cell cycle time was split up into interphase and mitosis for wild type (dark and light blue bars) and *wdr62* mutant (*wdr62*$^{\Delta 3\text{-}9}$*/Df(2L)Exel8005;* dark and light green bars) neuroblasts. **(F)** Cell cycle length (interphase and mitosis) measured for wild type **(F)** and **(G)** *wdr62* (*wdr62*$^{\Delta 3\text{-}9}$*/Df(2L)Exel8005*) mutant neuroblasts, all of which showing the centrosome asymmetry phenotype. Thin lines represent individual neuroblasts (blue; wild type, green; *wdr62* mutants) and the thicker bar on top denotes the average cell cycle time. For all panels, number of scored neuroblasts is indicated in brackets (n's). Error bars correspond to standard error of the mean (SEM). ***; $p < 0.0001$. **; $p < 0.001$, *; $p < 0.05$. n.s; not significant. Scale bar is 20 μm.

Supplemental movies

Movie 1: wild type neuroblasts maintain an active MTOC tethered to the apical cortex, related to Figure 1
Wild type larval neuroblast expressing the centriolar marker DSas4::GFP (green) and the MTOC marker Cherry::Jupiter (white). Note that after centrioles separate (starting at 0:02:57), one centriole remains tethered to the apical cortex, maintaining an active MTOC. The mother centriole-containing centrosome downregulates MTOC activity, regaining it only at prophase (starting at 0:17:42). The neuroblast was imaged every 59s. Time scale is h:mm:ss:ms. The scale bar is 3 μm.

Movie 2: *wdr62* mutants downregulate MTOC activity on the apical centrosome, related to Figure 1
wdr62 mutant larval neuroblast expressing the centriolar marker DSas4::GFP (green) and the MTOC marker Cherry::Jupiter (white). Note that the apical centriole loses the MTOC marker Cherry::Jupiter and moves away from the apical cortex. Maturation starts at 1:44:26. The neuroblast was imaged every 118s. Time scale is h:mm:ss:ms. The scale bar is 4 μm.

Movie 3: Wild type centrosomes maintain γ-Tubulin on the active MTOC throughout the cell cycle, related to Figure 1
Wild type larval neuroblast expressing the PCM marker γ-Tub::GFP (green in merged movie on the left; green in single channel movie on the right) and the MTOC marker Cherry::Jupiter (white; left movie). Note that the apical MTOC maintains γ-Tub::GFP throughout the cell cycle. The neuroblast was imaged every 57s. Time scale is h:mm:ss:ms. The scale bar is 2 μm.

Movie 4: *wdr62* mutant neuroblasts downregulate γ-Tubulin on the active MTOC during interphase, **related to Figure 1**
wdr62 mutant larval neuroblast expressing the PCM marker γ-Tub::GFP (green in merged movie on the left; green in single channel movie on the right) and the MTOC marker Cherry::Jupiter (white; left movie). Note that the apical MTOC downregulates γ-Tub::GFP and Cherry::Jupiter significantly during interphase. Maturation starts simultaneously on both centrosomes (~2:36:29). The neuroblast was imaged every 89s. Time scale is h:mm:ss:ms. The scale bar is 2 μm.

Movie 5: Wild type centrosomes maintain Polo on the active MTOC throughout the cell cycle, **related to Figure 2**
Wild type larval neuroblast expressing Polo::GFP (green in merged movie on the left; green in single channel movie on the right) and the MTOC marker Cherry::Jupiter (white; left movie). Note that the apical MTOC maintains Polo::GFP throughout the cell cycle. The neuroblast was imaged every 47s. Time scale is h:mm:ss:ms. The scale bar is 2 μm.

Movie 6: *wdr62* mutant neuroblasts downregulate Polo from the active MTOC, **related to Figure 2**
wdr62 larval neuroblast expressing Polo::GFP (green in merged movie on the left; green in single channel movie on the right) and the MTOC marker Cherry::Jupiter (white; left movie). Note that the apical MTOC downregulates Polo::GFP during interphase concomitantly with cherry::jupiter and loses its position on the apical cortex. The neuroblast was imaged every 90s. Time scale is h:mm:ss:ms. The scale bar is 2 μm.

Movie 7: *polo*^{1} mutant neuroblasts downregulate MTOC activity on apical centrosome, related to Figure 2
polo^{1} mutant larval neuroblast expressing the centriolar marker DSas4::GFP (green) and the MTOC marker Cherry::Jupiter (white). Note that the apical centriole loses the MTOC marker Cherry::Jupiter and moves away from the apical cortex. Maturation starts normally at 1:11:02. The neuroblast was imaged every 118s. Time scale is h:mm:ss:ms. The scale bar is 3 μm.

Supplemental Experimental Procedures

Fly strains and genetics: All mutant chromosomes were balanced over CyO actin::GFP or TM6B, Tb. The following fly strains were used: Oregon-R (wild type), *Df(2L)Exel8005,* (a deficiency removing the entire *wdr62* locus and adjacent genes; Bloomington stock center), *polo*^{1} (Sunkel and Glover, 1988), *cnb* RNAi (v28651; VDRC), *wdr62*$^{\Delta 2a}$, *wdr62*$^{\Delta 3\text{-}9}$ (this work), *zeste-white 10* (Bloomington stock center). Until otherwise noted, mutants were crossed over the corresponding deficiency and analyzed in a heteroallelic combination. Transgenes and fluorescent markers: *pUbq-DSas4::GFP* (Peel et al., 2007), *pUbq-Cnb::YFP* (Januschke et al., 2013), *pUASp-YFP-cnb::PACT* (Januschke et al., 2013), *worGal4, pUAST-cherry::Jupiter* (Cabernard and Doe, 2009), *ncd-γ-Tub::EGFP* (Hallen et al., 2008), *polo::GFP*^{CC01326} (protein trap line; (Buszczak et al., 2007)).

Generation of *wdr62* alleles: *wdr62*$^{\Delta 2a}$: the piggyBac insertion line *PBac{PB}CG7337(c04508)* and *PBac{PB}CG7337(c04728)* (Exelixis) were crossed to *hsFlp* and the resulting progeny was heat shocked at 37°C to induce Flipase activity according to previously published protocols (Thibault et al., 2004). *wdr62*$^{\Delta 3\text{-}9}$*:* Target-specific sequences with high efficiency were chosen using the CRISPR optimal target finder (http://tools.flycrispr.molbio.wisc.edu/targetFinder/) and DRSC CRISPR Efficiency Predictor web tools (http://www.flyrnai.org/evaluateCrispr/). These sequences were then cloned into pU6-BbsI-chiRNA (Gratz et al., 2013). To generate the replacement donor, 1kb homology arms flanking the target sequences at 5' and 3' ends were cloned into pHD-DsRed-attP. Flies expressing *nos-Cas9* (Ren et al., 2013) were injected with 5' and 3' specific target chiRNA and the replacement donor vector. Successful mutagenesis was detected by screening for DsRed+ eyes. Constitutively active Cre (Bloomington stock center) was crossed in to remove the DsRed marker.

Generation of *wdr62::GFP* and *cnn::mCherry* MiMIC lines: *Mi{MIC}-CG7337(MI0770)* and *Mi{MIC}-cnn(MI08383)* (Venken et al., 2011) was crossed to phiC31 integrase (expressed under the vasa promotor; Bloomington stock center) and the resulting progeny were injected with GFP and mCherry exchange cassettes, respectively (Venken et al., 2011). Positive lines were initially screened for loss of yellow body marker and the orientation of the insert was checked by PCR.

Generation of transgenic lines: Generation of *pUASt-wdr62RA::mDendra2*: *wdr62-RA* was PCR amplified from the full length cDNA (DGRC clone LD01189) and cloned into *pUASt-attB* using Kpn1 and Not1. The construct was injected into attP(VK00033) (Venken et al., 2006) flies. *pUbq-Cnb::YFP* and *cnn::mCherry* were recombined onto *wdr62*$^{\Delta 2a}$ using standard genetic procedures. All UAS transgenes were expressed using *worGal4* (Albertson and Doe, 2003).
Generation of *polo::mDendra2: Polo::mDendra2* was cloned into *pattB* vector using In-Fusion Multiple fragment cloning (Clontech). *Polo 5'UTR* and *mDendra2* were PCR amplified and inserted between XhoI and NdeI restriction site, followed by inserting PCR amplified *Polo* coding and *Polo 3'UTR* between NdeI and BamHI restriction sites. *pattB-polo::mDendra* was injected into attP40 and attP(VK00027) landing sites (Genetic Services).

Antibodies used: The following primary antibodies were used: rabbit anti-aPKC (1:1000; Santa Cruz Biotechnology), mouse anti-γ-tub (Sigma; 1:500), guinea pig anti-Deadpan (1:1000, gift from J. Skeath), rat anti-α-Tub (Serotec; 1:1000), mouse anti-Discs large (1:100; Developmental Study Hybridoma Bank (DSHB)), mouse anti-α-Tub (DM1A, Sigma; 1:2500), guinea-pig anti-Bazooka (1:1000), rat anti-Pins (1:400) (gift from Fumio Matsuzaki), mouse anti-Pros (1:1000), rat and guinea-pig anti-Mira (1:500) (gifts from Chris Doe), rabbit anti-Numb (1:100; gift from J. Knoblich), rabbit anti-Asl (1:500), rabbit anti-Plp (1:1000; gift from N. Rusan), rabbit anti-Sas4 (1:250), rabbit anti-Cnn (1:1000) (gifts from J. Raff). Secondary antibodies were from Molecular Probes and the Jackson Immuno laboratory.

Immunostainings: 96-120h (AEL; after egg laying) larval brains were dissected in Schneider's medium (Sigma) and fixed for 20 min in 4% paraformaldehyde in PEM (100mM PIPES pH 6.9, 1mM EGTA and 1mM $MgSO_4$). After fixing, the brains were washed with PBSBT (1X PBS, 0.1% Triton-X-100 and 1% BSA) and then blocked with 1X PBSBT for 1h. Primary antibody dilution was prepared in 1X PBSBT and brains were incubated overnight at 4 °C. Brains were washed with 1X PBSBT four times for 20 minutes each and then incubated with secondary antibodies diluted in 1X PBSBT at 4 °C overnight. The next day, brains were washed with 1X PBST (1x PBS, 0.1% Triton-X-100) four times for 20 minutes each and kept in Vectashield (Vector laboratories) mounting media at 4 °C. For brain size stainings, embryo collections were done every 4 hours and the larvae were incubated at 25°C until 120h AEL.
Image Acquisition: Fixed samples were imaged using an inverted Leica TSC SPE confocal microscope. For representative images a 60X/1.40NA oil immersion objective was used. For 4X scans a z-step size of 0.3 µm and

for 1X scans a z-step size of 1.0 µm was used. Live samples were imaged with an Andor revolution spinning disc confocal system, consisting of a Yokogawa CSU-X1 spinning disk unit and two Andor iXon3 DU-897-BV EMCCD cameras. A 60X/1.4NA oil immersion objective mounted on a Nikon Eclipse Ti microscope was used for most images. Live imaging voxels sizes are 0.22 X 0.22 X 0.5µm (60x/1.4NA spinning disc).

Live imaging sample preparation: 5ml Schneider's insect medium (Sigma-Aldrich S0146) was mixed with 5µL of 0.5M ascorbic acid (Sigma-Aldrich A4034) and 50µL of HyClone bovine growth serum (Thermo Scientific SH3054102) immediately before use and warmed up to room temperature. This imaging medium was supplemented with fat bodies of ~ 10 *yw* third instar larvae. 96-120hr AEL old mutant or wild type larval brains were dissected in imaging medium. The dissected brains, along with fat bodies, were transferred onto a gas-permeable membrane (YSI Life Sciences 5793), fitted on a metallic slide. Brains were oriented with the brain lobes facing the coverslip. Excess media was removed until the brain lobes were in contact with the coverslip. The sample was sealed with Vaseline (Cabernard and Doe, 2013).

Super–Resolution 3D Structured Illumination Microscopy (3D-SIM): 3D-SIM was performed on fixed brain samples using a DeltaVision OMX-Blaze system (version 4; Applied Precision, Issaquah, WA), equipped with 405, 445, 488, 514, 568 and 642 nm solid-state lasers. Images were acquired using a Plan Apo N 60x, 1.42 NA oil immersion objective lens (Olympus) and 4 liquid-cooled sCMOs cameras (pco Edge, full frame 2560 x 2160; Photometrics). Exciting light was directed through a movable optical grating to generate a fine-striped interference pattern on the sample plane. The pattern was shifted laterally through five phases and three angular rotations of 60° for each z section. Optical z-sections were separated by 0.125 µm. The laser lines 488, 568 and 642 nm were used for 3D-SIM acquisition. Exposure times were typically between 3 and 100 ms, and the power of each laser was adjusted to achieve optimal intensities of between 5,000 and 8,000 counts in a raw image of 15-bit dynamic range at the lowest laser power possible to minimize photobleaching. Multichannel imaging was achieved through sequential acquisition of wavelengths by separate cameras.

Definition of interphase and mitosis time and calculation of cell cycle length:
Interphase was defined as the time window from the end of telophase until prophase, when centrosome maturation set in, manifested in the appearance of the basal MTOC. Mitosis was defined as the window from prophase until the end of telophase. The spindle/MTOC marker Cherry::Jupiter was used to determine the different cell cycle stages. Whenever possible, neuroblasts were also considered undergoing two divisions within the time span of the movie recordings. In these instances, cell cycle times were measured from two repeating and recognizable cell cycle stages (e.g metaphase 1 – metaphase 2).

Detection and counting of neuroblasts: We dissected carefully staged wild type, *cnb* RNAi expressing (v28651; VDRC) and $wdr62^{\Delta 2a}$ mutant third instar larvae (120h after egg laying) and stained with the neuroblast markers Deadpan (Dpn) and Discs large 1 (Dlg1). Dpn^{+} neuroblasts were counted in 3D reconstructions using Imaris imaging software (spot function).
cnb was knocked-down by crossing the neuroblast specific worniu-Gal4 (worGal4) driver (Albertson and Doe, 2003) to v28651. WorGal4 turns on in the embryonic CNS and is also active in all larval stages.

3D-SIM Image Reconstruction: Raw 3D-SIM images were processed and reconstructed using the DeltaVision OMX SoftWoRx software package (Applied Precision; (Gustafsson, 2000)). The resulting size of the reconstructed images was of 512 x 512 px from an initial set of 256 x 256 raw images. The channels were aligned in the image plane and around the optical axis using predetermined shifts as measured using a target lens and the SoftWoRx alignment tool. The channels were then carefully aligned using alignment parameter from control measurements with 0.5 µm diameter multi-spectral fluorescent beads (Invitrogen, Molecular Probes).

Image processing and calculations: Images were processed using Imaris x64 7.5.2 and Fiji. Andor IQ2 files were converted into Imaris files using a custom-made Matlab code. Centrosomes were tracked in live and fixed samples using the spot tool in Imaris, which calculated the mean intensities specific to where the spot was placed. Asymmetry indices were calculated by dividing the apical centrosome to the basal centrosome. To calculate the position of each centrosome during maturation in live samples, the angle of each maturing centrosome, using the cell center as the reference point in relation to the future division axis, was calculated. Spindle orientation in fixed samples was measured by determining the coordinates of the center of maximum intensity of apical and basal crescents, respectively. These coordinates were used to calculate a polarity axis vector. Spindle axis vector were calculated using similar methods. Custom-made Matlab codes were used to calculate the angle between polarity and spindle vectors in 3D. The spindle orientation correction factor was determined from live imaging experiments by calculating the angle between two spindle vectors: (1) a spindle vector at the beginning of metaphase and (2) the spindle vector at the end of metaphase, respectively. Brain volumes were calculated in fixed samples by manually

generating a surface on the brain lobe using the surface tool in Imaris. Intensity profiles of centrosomes and MTs were generated in Fiji. Maximum intensity projections were generated and a line was used to measure the intensity at the centriole position. Using a Macro, this line was duplicated onto the channel to be measured. Pictures were assembled in Adobe Illustrator CS6. Quantifications and graphical representations were generated in Microsoft Excel.
3D SIM Image Analysis: The reconstructed images were converted to OME-TIFF files and 3D heat plots were generated using a custom made MATLAB code. Representative images were taken in Imaris after interpolation.

Definition of apical and basal centrosome
Apical and basal centrosomes are distinguished based on two criteria: (1) we experimentally determined in *wdr62* mutants that the Cnb^{+} centriole maintains MTOC activity longer than the Cnb^{-} centrosome. Since the apical centrosome contains the Cnb^{+} centriole in wild type neuroblasts, we therefore consider the centrosome maintaining MTOC for a longer time to be the apical centrosome. (2) We experimentally determined that apical centrosomes in interphase neuroblasts contain more Polo in both wild type and *wdr62* mutants.

Supplemental References

Albertson, R., and Doe, C.Q. (2003). Dlg, Scrib and Lgl regulate neuroblast cell size and mitotic spindle asymmetry. Nat. Cell Biol. *5*, 166–170.

Buszczak, M., Paterno, S., Lighthouse, D., Bachman, J., Planck, J., Owen, S., Skora, A.D., Nystul, T.G., Ohlstein, B., Allen, A., et al. (2007). The carnegie protein trap library: a versatile tool for Drosophila developmental studies. Genetics *175*, 1505–1531.

Cabernard, C., and Doe, C.Q. (2013). Live Imaging of Neuroblast Lineages within Intact Larval Brains in Drosophila. Cold Spring Harbor Protocols *2013*, 970–977.

Cabernard, C., and Doe, C.Q. (2009). Apical/basal spindle orientation is required for neuroblast homeostasis and neuronal differentiation in Drosophila. Dev. Cell *17*, 134–141.

Gratz, S.J., Cummings, A.M., Nguyen, J.N., Hamm, D.C., Donohue, L.K., Harrison, M.M., Wildonger, J., and O'Connor-Giles, K.M. (2013). Genome engineering of Drosophila with the CRISPR RNA-guided Cas9 nuclease. Genetics *194*, 1029–1035.

Gustafsson, M.G.L. (2000). Surpassing the lateral resolution limit by a factor of two using structured illumination microscopy. J Microsc *198*, 82–87.

Hallen, M.A., Ho, J., Yankel, C.D., and Endow, S.A. (2008). Fluorescence recovery kinetic analysis of gamma-tubulin binding to the mitotic spindle. Biophys. J. *95*, 3048–3058.

Januschke, J., Reina, J., Llamazares, S., Bertran, T., Rossi, F., Roig, J., and Gonzalez, C. (2013). Centrobin controls mother–daughter centriole asymmetry in Drosophila neuroblasts. Nat. Cell Biol. *15*, 241–248.

Peel, N., Stevens, N.R., Basto, R., and Raff, J.W. (2007). Overexpressing centriole-replication proteins in vivo induces centriole overduplication and de novo formation. Curr. Biol. *17*, 834–843.

Ren, X., Sun, J., Housden, B.E., Hu, Y., Roesel, C., Lin, S., Liu, L.-P., Yang, Z., Mao, D., Sun, L., et al. (2013). Optimized gene editing technology for Drosophila melanogaster using germ line-specific Cas9. Proceedings of the National Academy of Sciences *110*, 19012–19017.

Sunkel, C.E., and Glover, D.M. (1988). polo, a mitotic mutant of Drosophila displaying abnormal spindle poles. Journal of Cell Science *89 (Pt 1)*, 25–38.

Thibault, S.T., Singer, M.A., Miyazaki, W.Y., Milash, B., Dompe, N.A., Singh, C.M., Buchholz, R., Demsky, M., Fawcett, R., Francis-Lang, H.L., et al. (2004). A complementary transposon tool kit for Drosophila melanogaster using P and piggyBac. Nat Genet *36*, 283–287.

Venken, K.J.T., He, Y., Hoskins, R.A., and Bellen, H.J. (2006). P[acman]: a BAC transgenic platform for targeted insertion of large DNA fragments in D. melanogaster. Science *314*, 1747–1751.

Venken, K.J.T., Schulze, K.L., Haelterman, N.A., Pan, H., He, Y., Evans-Holm, M., Carlson, J.W., Levis, R.W., Spradling, A.C., Hoskins, R.A., et al. (2011). MiMIC: a highly versatile transposon insertion resource for engineering Drosophila melanogaster genes. Nat. Methods *8*, 737–743.